For submission to Nature as a letter

3 February 2014

Cosmogenic ^{10}Be records 10 million years of Greenland Ice Sheet history

Paul Bierman, Department of Geology and Rubenstein School of the Environment and Natural Resources, University of Vermont, Burlington, VT 05405, pbierman@uvm.edu, 802 656 4411

Jeremy D. Shakun, Department of Earth and Environmental Sciences, Boston College, Chestnut Hill, MA 02467, jeremy.shakun@bc.edu, 617 552 1625

Long records of ice sheet behavior are critical for understanding cryospheric response to climate change. Clastic marine sediments preserve material eroded from the continents, allowing the development of time-series that quantify the growth of ice sheets and the character of now-eroded landscapes. Sediment from non-glaciated landmasses typically contains high concentrations of the cosmogenic nuclide ^{10}Be, the result of near-surface exposure to cosmic rays. In contrast, ice sheet cover prevents cosmogenic nuclide production and erodes material containing nuclides produced before glaciation, decreasing the concentration of ^{10}Be in sediment carried by ice. The Cenozoic growth and erosion history of the Greenland Ice Sheet is poorly constrained. Here we use a record of *in-situ*-produced ^{10}Be in detrital sediment from a marine core off the southeast coast of Greenland to decipher the

long-term history of the Greenland Ice Sheet. The ten-fold drop in the ^{10}Be concentration of Greenland-derived quartz between 10 and 3 million years ago reflects aerially-limited Miocene and Pliocene glaciers and progressive erosion of material containing ^{10}Be produced before glaciation. A spike in ^{10}Be concentration ~ 2.5 million years ago may indicate continent-wide expansion of the ice sheet, coincident with the onset of Northern Hemisphere glaciation inferred from marine oxygen isotope and ice-rafted debris records. A four-fold decrease in ^{10}Be concentration across the mid-Pleistocene transition reflects either the final removal of pre-glacial regolith or intensification of glaciation. By about 800,000 years ago, ^{10}Be concentration in core sediment is indistinguishable from that of sediment exported by the ice sheet today, suggesting that the ice sheet has been generally large and stable since then. This approach could be useful to reconstructing the history of other ice sheets.

The long-term history of large ice sheets has been interpreted by analysis of marine sediment cores, which preserve in their physical, chemical, and isotopic stratigraphy a record of Earth history and both surface and marine processes[1,2]. However, relatively few proxies provide a direct, quantitative, and large-scale indicator of the variability of individual ice sheets[3]. Such information is critical to establishing the sensitivity of ice sheets to climate change, which is the largest source of uncertainty in future projections of sea level rise. For example, estimates of the global warming threshold that would eventually eliminate the Greenland Ice Sheet range from 1 to 5°C [4].

Continental glaciation of Greenland is typically thought to have begun near the onset of Northern Hemisphere glacial cycles at ~ 2.7 Ma inferred from marine oxygen isotope and ice-rafted debris (IRD) records[5-7]. Some marine and modeling data, on the other hand, suggest that initial ice mass growth in Greenland, albeit of uncertain size, commenced from 5 to 25 million years earlier[8-10]. It is also unclear how Greenland glaciation evolved once the ice sheet was established, for instance, across the mid-Pleistocene transition[11].

Beryllium-10 is produced in near-surface rock and soil primarily by the bombardment of cosmic-ray neutrons. At depths below several meters of rock, isotope production rates are much lower and production is dominated by the interaction of muons[12]. Continental sediment usually contains >100,000 atoms g^{-1} of *in-situ* produced ^{10}Be, the result of subaerial exposure to cosmic rays[13]. On a steadily eroding, ice-free landscape, the concentration of ^{10}Be in sediment can be interpreted as an erosion rate assuming the elevation and latitude of the sediment source is known[14]. Once Earth's surface is covered by glacial ice, ^{10}Be production ceases and glacial erosion removes the most highly-dosed, near-surface material first before excavating material at depth containing progressively less ^{10}Be.

After the start of glaciation, the concentration of ^{10}Be in marine sediment sourced from Greenland is controlled by the ^{10}Be concentration of material eroded by the ice sheet from its bed and transported to the coast (Figure 1). The ^{10}Be concentration on the bed is controlled both by the pre-glacial spatial and depth distribution of isotope production and by the landscape erosion rate, and, after glaciation begins, by the rate of sub-ice erosion, the time since the bed was covered by ice and nuclide production ceased, and the duration and extent of sub-aerial landscape exposure during interglacial periods, when ice-sheet area is reduced, perhaps dramatically.

In order to understand the glacial erosion history of Greenland, we measured *in situ*-produced ^{10}Be in 30 quartz sand samples from the top 554 m of Ocean Drilling Program site 918 (63.1°N, 38.6°W, 1800 m depth), located in the Irminger basin, 110 km southeast of Greenland (Figure 2). This site is adjacent to the more dynamic southern portion of the Greenland Ice Sheet, as suggested by modeling of the ice sheet (Figure 2)[15,16] and thus is well situated to record past ice sheet variability. Site 918 was previously used to define the onset of Greenland glaciation at roughly 7 Ma based on the earliest occurrence of IRD in the core[10]; this IRD is included in our oldest sample. The stratigraphy and core location suggest much of the sediment at the coring site was deposited directly from suspension or by rain-out of IRD[10]; some of the sediment was deposited by mass flows but several lines of argument suggest that the quartz we measured is dominantly of Greenlandic origin, including the proximity of the core to Greenland; currents in the area drift ice from northeast Greenland (Figure 2); site 918 is well north of the heart of the Laurentide IRD belt as reflected in Heinrich layers[17]; downcore IRD is similar to modern Greenland IRD[10]; site 919 located only 70 km further offshore than 918 contains >90% less sand[10]; and sediment from nearby Iceland contains no quartz.

To estimate ^{10}Be concentration at the time of sediment deposition, we decay-corrected[18] (^{10}Be $t_{1/2}$ = 1.387 Myr) measured ^{10}Be concentrations using the core age model (Figures 3, 4). The chronology is anchored to the paleomagnetic timescale over the Pleistocene, but less well constrained by strontium isotope and biostratigraphy in the

Pliocene and Miocene (Figure 3a). Age model uncertainties can alter the absolute value of decay-corrected ^{10}Be concentrations and change the timing of some isotopic shifts, but have minimal impact on the overall structure of the record (Figure 4b).

Measured ^{10}Be concentrations are low, 2100 to 40,000 atoms g^{-1} (Figure 3b, Supplementary Information, Table 1). Decay-corrected concentrations are highest in the oldest sediment (~10 Ma according to the age model, 470,000 ± 38,000 atoms g^{-1}) and generally decrease over time (Figure 4b). Inverting the ^{10}Be data from the oldest sediment sample and assuming that the sediment delivered to the deep ocean as IRD was stripped by glaciers at an elevation near sea-level suggests a landscape-averaged pre-glacial Greenland denudation rate of about 7±1 m/My, lower than basin-scale erosion rates for polar climates but higher than polar rates of outcrop erosion[13].

By the late Pliocene, ^{10}Be concentrations are more than an order of magnitude lower than at the beginning of the record, reaching a minimum of 12,000 atoms g^{-1} at 2.7 Ma. We interpret this decrease as progressive glacial erosion of once-stable Tertiary regolith over limited areas of Greenland, perhaps by valley glaciers or ice caps with calving margins (Figure 1b). A general increase in the intensity and/or aerial cover of glaciation is supported by rising concentrations of coarse sediment over the length of the core (Figure 4a)[10].

At the dawn of the Pleistocene, the ^{10}Be concentration abruptly increased (Figure 4b). One sample, including sediment deposited at 2.5 Ma, had nearly 150,000 atoms/g of ^{10}Be when it was deposited, a concentration more similar to Miocene-age sediment than to any Quaternary age material. This ^{10}Be-rich quartz may have been eroded from previously unglaciated areas of Greenland and thus reflects the first continent-wide glaciation, an interpretation consistent with the abundance of IRD found at site 918 at this time[10]. Alternatively, this pulse of ^{10}Be enriched sediment could record a major and long-lasting deglaciation event. One such early interglacial, ~2.4 Ma, could be represented by the Kap København Formation in northern Greenland which contains flora and fauna indicative of relatively warm climates. However, this formation is thought to have been deposited in <20,000 years[19], not sufficiently long to explain the magnitude of the ^{10}Be spike. Between 2.5 Ma and 0.8 Ma, the decay-corrected concentration of ^{10}Be generally declines (Figure 4b)[20]. The Pleistocene decline in ^{10}Be concentration is consistent with progressive stripping of the preglacial landscape by sub-ice erosion during the Quaternary. As sediment and rock are removed from the landscape under the ice by erosion, material that was deeply shielded in pre-glacial times and thus less dosed by cosmic radiation is incorporated into basal ice and carried offshore before being deposited as IRD (Figure 1c).

An abrupt, four-fold drop in ^{10}Be concentration occurs across the mid-Pleistocene transition at 0.8 Ma (Figure 4b). There are several possible interpretations for this feature. First, if pre-glacial regolith still existed and was well-mixed beneath the ice sheet as till during the early Pleistocene, it would have had a fairly constant ^{10}Be concentration with depth. In this case, the decrease in ^{10}Be concentration at 0.8 Ma may reflect near complete export of regolith and a switch to erosion of bedrock, which would have contained less ^{10}Be than the regolith. The timing of this substrate change, if it also occurred in North America, would be consistent with the regolith hypothesis for the mid-Pleistocene transition from 41 to 100-kyr glacial cycles, which posits that thinner, more responsive ice sheets sliding on regolith transitioned to larger, more sluggish ice sheets resting on bedrock[21]. Or, an increase in the erosivity of the Greenland Ice Sheet during the mid-Pleistocene transition could have reduced ^{10}Be concentrations as deeper-sourced material was rapidly exported. Lastly, the Greenland Ice Sheet may have deglaciated more frequently during the early Pleistocene than the late Pleistocene, helping to sustain higher ^{10}Be levels through repeated episodes of interglacial exposure. If correct, this latter interpretation suggests that the ice sheet may be susceptible to substantial retreat at CO_2 and temperature levels only slightly higher than the Holocene[3,22,23].

^{10}Be values over the past 0.8 My are similar to those in sediments issuing from the western, southern, and eastern Greenland Ice Sheet margin today[20] (Figure 4b), except for one brief spike in the mid-Brunhes, consistent with the existence of a large, modern-like Greenland ice sheet for most of the last million years. Given ^{10}Be surface production rates of atoms to tens of atoms per gram per year, loss of the ice sheet for more than a few thousand years should be detectable in the later Pleistocene marine record.

In situ produced ^{10}Be, derived from continental glacial erosion and preserved in marine sediment, records the development of initial glaciation on Greenland from ~10 to 3 Ma, the first growth of a full Greenland ice sheet at ~2.5 Ma, and a significant change in ice-sheet behavior at 0.8 Ma. The magnitude of the ^{10}Be signal as well its general consistency with other ice sheet and climate records suggests that our approach could provide a useful new tool for reconstructing other long-term ice-sheet histories.

Methods Summary

Core samples were obtained from the Bremen Core Repository. We disaggregated and wet-sieved sediments isolating the 0.125 to 0.75 mm grain size fraction and used weak acid ultrasonic leaching (0.5 to 0.25% HF and HNO_3) to slowly dissolve all minerals other than quartz[24]. We amalgamated quartz from subsamples taken over an interval of core until we had sufficient quartz mass (7.8 to 25.3 g) from which to extract and measure ^{10}Be reliably. Thus, samples represent the average ^{10}Be content of quartz present in core sections ranging in length from 0.6 to 91 m (median = 7 m). Age spans for samples range from 0.002 to 3.1 My. Samples were dissolved using HF in the presence of ^{9}Be carrier produced from beryl and processed in batches of 12 including 1 or 2 full process blanks. Isotopic measurements were made at Livermore National Laboratory and referenced to standard 07KNSTD3110 [25] assuming a ^{10}Be/^{9}Be ratio of 2850×10^{-15} (Supplementary Information, Table 1). The average blank ratio ($4.6 \pm 1.0 \times 10^{-16}$, n= 6) was subtracted from measured ratios (Supplementary Information, Table 2). Using the half-life[18] of ^{10}Be and the age model for site 918 (Supplementary Information, Table 3), we corrected the measured ^{10}Be concentrations for radio-decay since burial on the sea floor using the average age of the sediment in the sampled core interval. Replicate preparation of sample 918-17 (918-17X) indicates reproducibility within measurement uncertainty (Supplementary Information, Table 1).

References Cited

1 Bond, G. *et al*. Evidence for massive discharge of icebergs into the North Atlantic ocean during the last glacial period. *Nature* **360**, 245-249 (1992).

2 Shackleton, N. J. *et al*. Oxygen isotope calibration of the onset of ice-rafting and history of glaciation in the North Atlantic region. *Nature* **307**, 620-623 (1984).

3 Alley, R. B. *et al*. History of the Greenland Ice Sheet: paleoclimatic insights. *Quaternary Science Reviews* **29**, 1728-1756 (2010).

4 Gregory, J. M. & Huybrechts, P. Ice-sheet contributions to future sea-level change. *Philosophical Transactions of the Royal Society A: Mathematical, Physical and Engineering Sciences* **364**, 1709-1732 (2006).

5 Maslin, M. A., Li, X. S., Loutre, M. F. & Berger, A. The contribution of orbital forcing to the progressive intensification of Northern Hemisphere glaciation. *Quaternary Science Reviews* **17**, 411-426 (1998).

6 Mudelsee, M. & Raymo, M. E. Slow dynamics of the Northern Hemisphere glaciation. *Paleoceanography* **20**, PA4022, doi:10.1029/2005pa001153 (2005).

7 Shackleton, N. J. *et al*. Oxygen isotope calibration of the onset of ice-rafting and history of glaciation in the North Atlantic region. *Nature* **307**, 620-623 (1984).

8 DeConto, R. M. *et al*. Thresholds for Cenozoic bipolar glaciation. *Nature* **455**, 652-656 (2008).

9 Eldrett, J. S., Harding, I. C., Wilson, P. A., Butler, E. & Roberts, A. P. Continental ice in Greenland during the Eocene and Oligocene. *Nature* **446**, 176-179 (2007).

10 Larsen, H. C. *et al*. Seven million years of glaciation in Greenland. *Science* **264**, 952–955 (1994).

11 Thiede, J. *et al*. Millions of years of Greenland Ice Sheet history recorded in ocean sediments. *Polarforschung* **80**, 141-159 (2011).

12 Heisinger, B. *et al*. Production of selected cosmogenic radionuclides by muons. *Geochimica et Cosmochimica Acta* **66**, A558 (2002).

13 Portenga, E. & Bierman, P. R. Understanding Earth's eroding surface with ^{10}Be. *GSA Today* **21**, 4-10 (2011).

14 Lal, D. Cosmic ray labeling of erosion surfaces; in situ nuclide production rates and erosion models. *Earth and Planetary Science Letters* **104**, 424-439 (1991).

15 Alley, R. B., Clark, P. U., Huybrechts, P. & Joughin, I. Ice-sheet and sea-level changes. *Science* **310**, 456-460 (2005).

16 Lunt, D. J., Foster, G. L., Haywood, A. M. & Stone, E. J. Late Pliocene Greenland glaciation controlled by a decline in atmospheric CO_2 levels. *Nature* **454**, 1102-1105 (2008).

17 Hemming, S. R. Heinrich events: Massive late Pleistocene detritus layers of the North Atlantic and their global climate imprint. *Reviews of Geophysics* **42**, RG1005, doi:10.1029/2003rg000128 (2004).

18 Korschinek, G. *et al*. A new value for the half-life of ^{10}Be by Heavy-Ion Elastic Recoil Detection and liquid scintillation counting. *Nuclear Instruments and Methods in Physics Research B* **268**, 187-191 (2010).

19 Funder, S. *et al*. Late Pliocene Greenland - The Kap Kobenhavn Formation in north Greenland. *Bulletin of the Geological Society of Denmark*, 117-134 (2001).

20 Nelson, A. *Using in situ cosmogenic ^{10}Be as a sediment source tracer in Greenland's paraglacial environment* MS thesis, University of Vermont, (2013).

21 Clark, P. U. & Pollard, D. Origin of the Middle Pleistocene transition by ice sheet erosion of regolith. *Paleoceanography* **13**, 1–9 (1998).

22 Hansen, J. E. & Sato, M. in *Climate Change: Inferences from Paleoclimate and Regional Aspects* (eds A. Berger, Fedor Mesinger, & Djordje Sijacki) 21-48 (Springer, 2012).

23 Lawrence, K. T., Herbert, T. D., Brown, C. M., Raymo, M. E. & Haywood, A. M. High-amplitude variations in North Atlantic sea surface temperature during the early Pliocene warm period. *Paleoceanography* **24**, PA2218, doi:10.1029/2008pa001669 (2009).

24 Kohl, C. P. & Nishiizumi, K. Chemical isolation of quartz for measurement of *in-situ* -produced cosmogenic nuclides. *Geochimica et Cosmochimica Acta* **56**, 3583-3587 (1992).

25 Nishiizumi, K. *et al*. Absolute calibration of ^{10}Be AMS standards. *Nuclear Inst. and Methods in Physics Research, B* **258**, 403-413 (2007).

26 Jansen, E. *et al*. in *Climate Change 2007: The Physical Science Basis. Contribution of Working Group I to the Fourth Assessment Report of the Intergovernmental Panel on Climate Change* (eds S. Solomon *et al*.) 434-497 (Cambridge University Press, 2007).

27 Israelson, C. & Spezzaferri, S. in *Proceedings of the Ocean Drilling Program, Scientific Results* **152** (eds A.D. Saunders, H.C. Larsen, & S.W. Wise, Jr.) 233-241 (1998).

28 Fukuma, K. in *Proceedings of the Ocean Drilling Program, Scientific Results* **152** (eds A.D. Saunders, H.C. Larsen, & S.W. Wise, Jr.) 265-269 (1998).

29 Scholz, D. & Hoffmann, D. L. StalAge: An algorithm designed for construction of speleothem age models. *Quaternary Geochronology* **6**, 369-382 (2011)

30 Zachos, J., Pagani, M., Sloan, L., Thomas, E. & Billups, K. Trends, rhythms, and aberrations in global climate 65 Ma to present. *Science* **292**, 686-693 (2001).

Supplementary Information is linked to the online version of the paper at www.nature.com/nature.

Acknowledgements

Research supported by NSF ARC-1023191. A. Nelson prepared the samples. W. Shakun and M. E. Shakun helped with sediment processing. S. Zimmerman and R. Finkel provided AMS expertise. W. Hale and the Bremen Core Repository facilitated core sampling.

Author contributions

PB and JDS designed the experiment. JDS oversaw core sampling. PB oversaw laboratory work and made isotopic analyses. PB and JDS interpreted the data and wrote the paper.

Figure Legends

Figure 1. Conceptual model of ^{10}Be concentration. (**a**) Ice-free conditions prior to glaciation, high ^{10}Be-concentration material delivered to the ocean. (**b**) Mountain glaciation and ice cap development during the late Miocene and Pliocene, eroding and exporting progressively deeper, and thus ^{10}Be-poorer, material from these regions. (**c**)

Expansion of a full Greenland Ice Sheet during the Pleistocene, initially stripping previously exposed ^{10}Be-rich surface material, followed by progressively deeper and thus ^{10}Be-poorer material from Greenland. Intensity of shading corresponds to relative ^{10}Be concentrations in bedrock, regolith, and sediment.

Figure 2. Location map. ODP site 918 shown as black dot, modern ocean currents indicated by arrows, and contours on Greenland give ice sheet thickness during the last interglacial as simulated by a multi-model ensemble[26]. Stars show the locations of ^{10}Be measurements made on modern sediments[20].

Figure 3. Site 918 age model and measured ^{10}Be concentrations. (a) Age constraints from strontium isotope[27], paleomagnetic[28], and biostratigraphic[10] data. Age-depth curve (black line) and 2σ uncertainty (gray shading) were calculated using a published age model algorithm[29]. (b) Measured ^{10}Be concentrations with 1σ uncertainty (gray shading).

Figure 4. Site 918 decay-corrected ^{10}Be record. (**a**) Sand (>63 μm) fraction at site 918 by weight. Arrow points to lowest (oldest) sample (918-30) with IRD at site 918[10]. (**b**) Decay-corrected concentrations of *in situ* produced ^{10}Be measured in quartz isolated from site 918 assuming age model shown in Figure 3a. Gray lines show results of 1000 Monte Carlo simulations perturbing age model with chronological uncertainties and measured ^{10}Be concentrations with analytical uncertainties. Dotted black line gives the average ^{10}Be concentration of 62 modern ice-contact and fluvial sediment samples collected from three regions in southern Greenland[20]. (**c**) Global deep ocean $\delta^{18}O$, a proxy for global ice volume and deep ocean temperature[30].

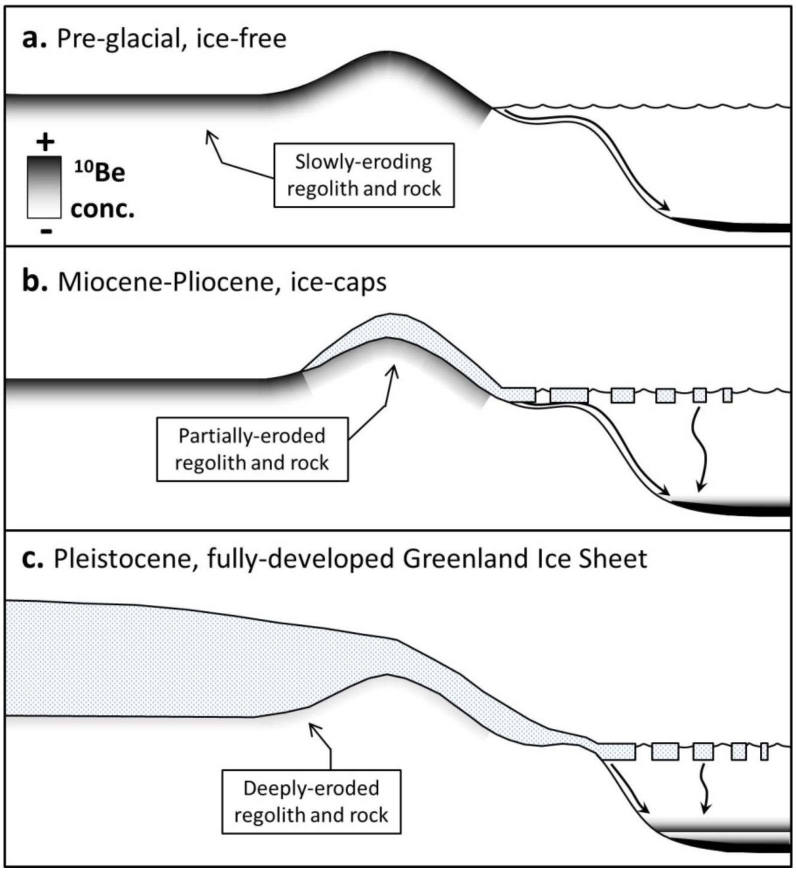

Figure 1. Bierman and Shakun

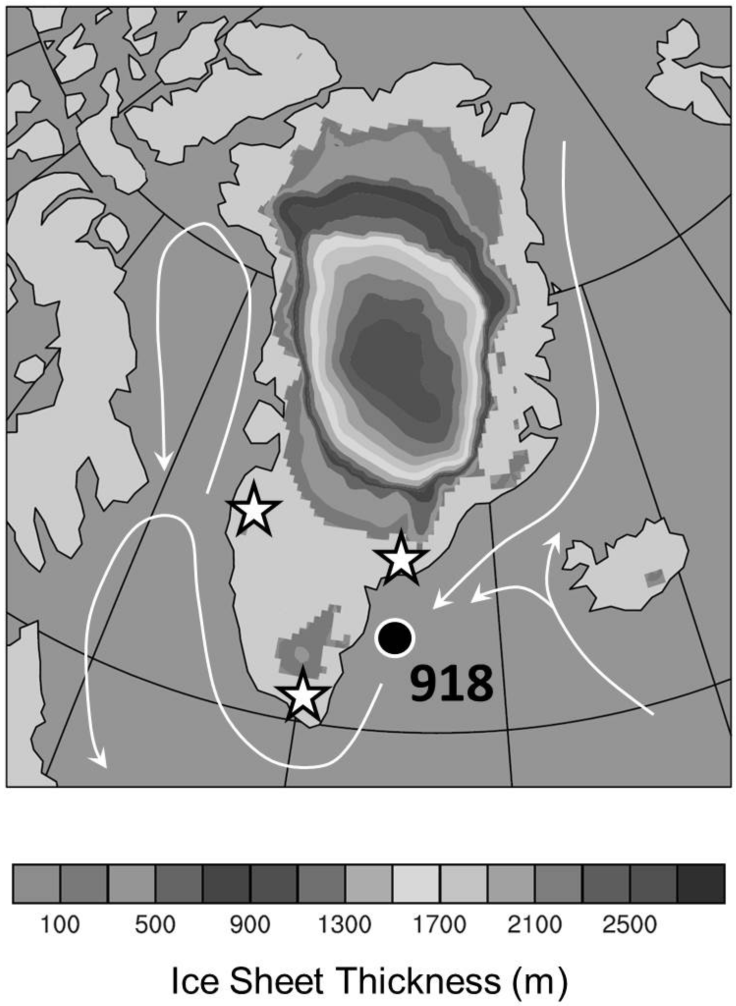

Figure 2. Bierman and Shakun

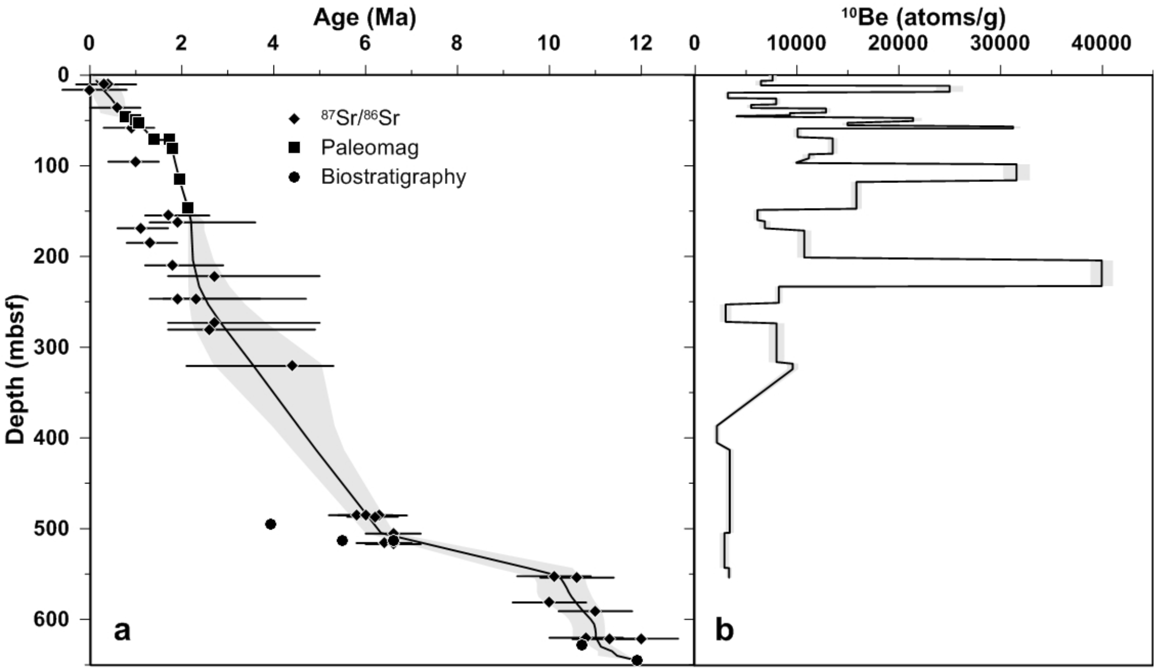

Figure 3. Bierman and Shakun

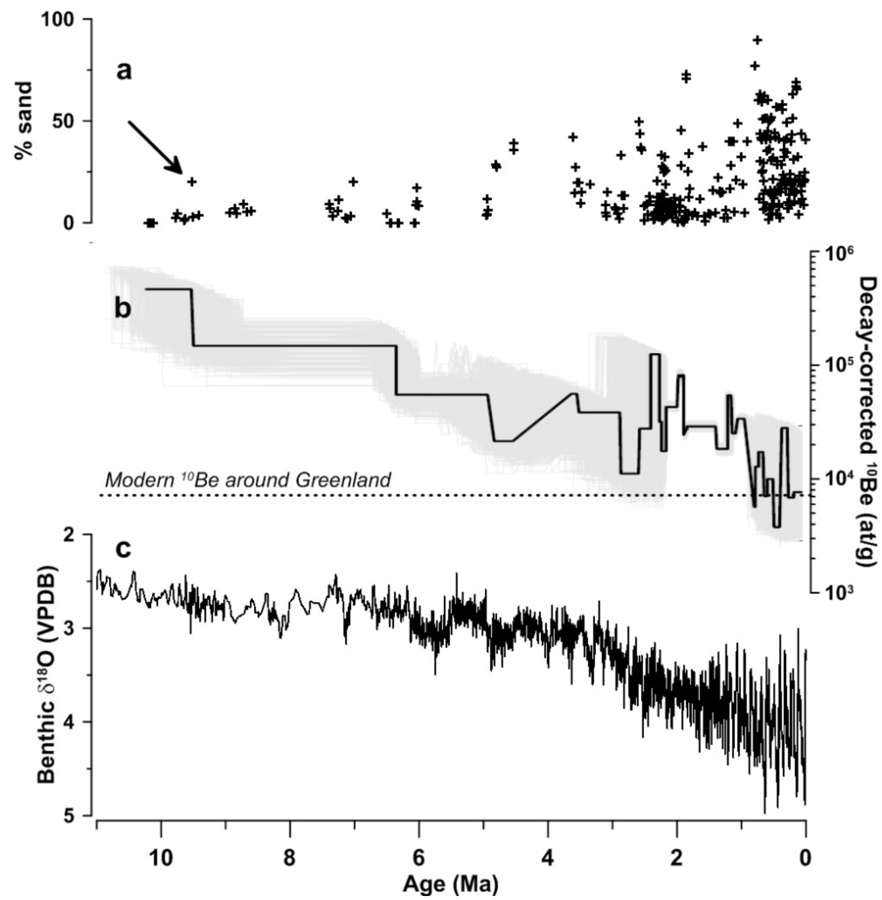

Figure 4. Bierman and Shakun

SUPPLEMENTRAY INFORMATION **TABLE 1.** Isotopic data and age model, Site 918

Sample	CAMS #	Top Depth (mbsf)	Bottom Depth (mbsf)	Top age (Ma)	Bottom age (Ma)	Blank corrected 10Be/9Be	quartz (g)	carrier 9Be (ug)	Measured 10Be (atoms/g)	Decay-corrected 10Be (atoms/g)
B504918-1	BE35206	0.5	6.1	0.012	0.141	8.44E-15 ± 4.47E-16	18.86	254.3	7601 ± 402	7898 ± 418
B507918-2	BE35234	6.3	11.3	0.149	0.224	9.32E-15 ± 7.72E-16	24.31	252.5	6463 ± 536	7095 ± 588
B504918-3	BE35207	11.9	18.5	0.249	0.331	2.77E-14 ± 1.47E-15	18.80	254.4	24991 ± 1325	28892 ± 1532
B507918-4	BE35235	19.4	25.4	0.367	0.456	3.05E-15 ± 2.70E-16	16.13	254.7	3211 ± 284	3944 ± 349
B504918-5	BE35208	25.8	32.3	0.475	0.558	1.14E-14 ± 5.65E-16	24.40	255.3	7958 ± 395	10302 ± 511
B507918-6	BE35237	32.8	36.3	0.561	0.615	6.27E-15 ± 4.56E-16	19.33	253.8	5494 ± 400	7372 ± 537
B507918-7	BE35238	36.9	41.3	0.625	0.689	1.86E-14 ± 6.30E-16	24.54	253.6	12849 ± 435	17843 ± 604
B505918-8	BE35211	41.8	44.3	0.691	0.745	8.17E-15 ± 4.05E-16	14.85	253.6	9308 ± 462	13326 ± 662
B507918-9	BE35239	45.0	45.6	0.748	0.762	4.17E-15 ± 3.13E-16	17.36	254.0	4072 ± 305	5938 ± 445
B505918-10	BE35212	47.3	50.6	0.911	1.019	1.96E-14 ± 7.71E-16	15.50	254.2	21409 ± 844	34676 ± 1367
B507918-11	BE35240	52.7	55.3	1.060	1.107	1.76E-14 ± 5.99E-16	19.93	254.2	14960 ± 510	25713 ± 876
B507918-12	BE35241	56.7	58.8	1.131	1.170	3.69E-14 ± 8.60E-16	19.96	252.9	31214 ± 728	55469 ± 1293
B505918-13	BE35213	59.0	68.3	1.172	1.339	1.48E-14 ± 6.00E-16	24.82	253.4	10063 ± 409	18849 ± 766
B505918-14	BE35214	69.7	86.7	1.363	1.811	1.65E-14 ± 5.89E-16	20.73	253.8	13501 ± 482	29842 ± 1065
B505918-15	BE35215	87.3	91.7	1.814	1.835	6.73E-15 ± 3.79E-16	10.22	254.1	11176 ± 630	27815 ± 1567
B505918-16	BE35216	96.3	96.9	1.857	1.859	1.33E-14 ± 5.12E-16	22.62	253.6	9939 ± 383	25157 ± 970
B505918-17	BE35217	98.3	116.0	1.866	1.953	2.59E-14 ± 7.60E-16	13.66	253.0	32054 ± 940	83251 ± 2441
B506918-17X	BE35233	98.3	116.0	1.866	1.953	2.19E-14 ± 1.01E-15	12.02	255.6	31072 ± 1432	80700 ± 3720
B505918-18	BE35218	117.8	147.3	1.964	2.137	1.84E-14 ± 6.16E-16	19.68	253.7	15833 ± 531	44114 ± 1479
B505918-19	BE35219	148.6	159.8	2.145	2.198	5.53E-15 ± 3.45E-16	15.31	254.0	6122 ± 382	18121 ± 1130
B506918-20	BE35222	161.1	168.8	2.201	2.206	4.90E-15 ± 4.11E-16	12.08	252.7	6841 ± 573	20573 ± 1724
B505918-21	BE35220	171.4	201.1	2.210	2.233	5.37E-15 ± 3.48E-16	8.49	253.6	10712 ± 693	32517 ± 2104
B506918-22	BE35224	204.3	232.5	2.242	2.369	2.64E-14 ± 7.34E-16	11.25	254.3	39927 ± 1108	126352 ± 3506
B506918-23	BE35225	233.2	251.0	2.378	2.551	1.25E-14 ± 5.70E-16	25.77	253.0	8217 ± 373	28157 ± 1279
B506918-24	BE35226	252.8	271.9	2.574	2.834	1.98E-15 ± 3.64E-16	11.23	253.9	2993 ± 549	11562 ± 2122
B506918-25	BE35227	273.6	316.3	2.856	3.499	5.12E-15 ± 4.95E-16	10.86	253.8	7990 ± 772	39103 ± 3779
B507918-26	BE35242	318.1	324.0	3.526	3.612	8.35E-15 ± 4.78E-16	14.78	254.1	9579 ± 549	57014 ± 3265
B506918-27	BE35228	386.6	405.2	4.529	4.806	3.36E-15 ± 4.55E-16	26.78	254.4	2134 ± 289	21993 ± 2976
B506918-28	BE35229	413.2	504.4	4.925	6.334	2.10E-15 ± 2.50E-16	10.47	253.9	3397 ± 404	56595 ± 6738
B506918-29	BE35230	504.7	543.1	6.334	9.491	1.32E-15 ± 2.11E-16	7.81	253.8	2875 ± 458	149907 ± 23874
B506918-30	BE35231	543.3	553.9	9.527	10.257	4.98E-15 ± 4.02E-16	25.30	253.4	3329 ± 269	466965 ± 37714

referenced to standard 07KNSTD3110[25] assuming a $^{10}Be/^{9}Be$ ratio of 2850 x 10^{-15}

Be extracted using the methods detailed in Corbett, L. Bierman, P., Graly, J., Neumann, T., Rood, D. (2013). Constraining landscape history and glacial erosivity using paired cosmogenic nuclides in Upernavik, Northwest Greenland. Geological Society of America Bulletin. v. 125, no. 9-10, 10.1130/B30813.1

SUPPLEMENTARY INFORMATION **TABLE 2.** Blank data, ^{10}Be

Sample	**CAMS #**	**Blank 10Be/9Be**	**carrier 9Be (ug)**
B504BLKX	BE35209	4.41E-16 ± 1.01E-16	253.9
B505BLK	BE35210	5.77E-16 ± 1.33E-16	251.7
B505BLKX	BE35221	3.39E-16 ± 1.44E-16	255.6
B506BLK	BE35223	3.91E-16 ± 9.66E-17	254.1
B507BLK	BE35236	5.81E-16 ± 1.49E-16	253.8
B506BLKX	BE35232	4.10E-16 ± 2.32E-16	253.4
	AVERAGE (1 SD)	4.57E-16 ± 1.00E-16	

referenced to standard 07KNSTD3110[25] assuming a $^{10}Be/^{9}Be$ ratio of 2850×10^{-15}

SUPPLEMENTARY INFORMATION **TABLE 3.** Age Model

Depth (mbsf)	Age (Ma)	error + (My)	error - (My)	Age constraint (**Paleomag**, **Biostrat**, **87Sr/86Sr**)	Reference
0	0			Assumed modern	
10.26	0.4	0.6	0.6	0.709173	Israelson and Spezzaferri, 1998
10.26	0.3	0.7	0.6	0.709178	Israelson and Spezzaferri, 1998
16.26	0	0.8	0.6	0.709183	Israelson and Spezzaferri, 1998
36.01	0.6	0.5	0.6	0.709166	Israelson and Spezzaferri, 1998
45.9	0.78			Brunhes/Matuyama	Fukuma, 1998
49	0.99			Jaramillo top	Fukuma, 1998
52.9	1.07			Jaramillo bottom	Fukuma, 1998
58.07	0.9	0.5	0.6	0.709153	Israelson and Spezzaferri, 1998
71.1	1.39			hiatus	Fukuma, 1998
71.1	1.73			hiatus	Fukuma, 1998
81	1.79			Olduvai top	Fukuma, 1998
95.45	1	0.5	0.6	0.709145	Israelson and Spezzaferri, 1998
115.1	1.95			Olduvai bottom	Fukuma, 1998
146.8	2.14			Reunion top	Fukuma, 1998
154.77	1.7	0.9	0.5	0.709107	Israelson and Spezzaferri, 1998
162.41	1.9	1.7	0.6	0.709098	Israelson and Spezzaferri, 1998
162.41	1.9	1.7	0.6	0.709098	Israelson and Spezzaferri, 1998
168.76	1.1	0.6	0.5	0.709137	Israelson and Spezzaferri, 1998
184.97	1.3	0.6	0.5	0.709126	Israelson and Spezzaferri, 1998
209.67	1.8	1.1	0.6	0.709102	Israelson and Spezzaferri, 1998
221.55	2.7	2.3	1	0.709076	Israelson and Spezzaferri, 1998
246.57	1.9	1.8	0.6	0.709097	Israelson and Spezzaferri, 1998
246.57	2.3	2.4	0.7	0.709107	Israelson and Spezzaferri, 1998
273.06	2.7	2.3	1	0.709076	Israelson and Spezzaferri, 1998
280.47	2.6	2.3	0.9	0.709077	Israelson and Spezzaferri, 1998
320.56	4.4	0.9	2.3	0.709083	Israelson and Spezzaferri, 1998
485.15	5.8	0.6	0.6	0.709009	Israelson and Spezzaferri, 1998
485.15	6	0.6	0.6	0.709018	Israelson and Spezzaferri, 1998
485.4	6.3	0.6	0.6	0.709004	Israelson and Spezzaferri, 1998
486.9	6.2	0.5	0.6	0.709011	Israelson and Spezzaferri, 1998
495	3.94			Last occurrence R. gelida	Larsen, 1994
505.39	6.6	0.6	0.6	0.708992	Israelson and Spezzaferri, 1998
513	5.5			Last occurrence D. quinqueramus	Larsen, 1994
513	6.6			N. atlantica coiling chance (D to S)	Larsen, 1994
515.83	6.4	0.6	0.6	0.708979	Israelson and Spezzaferri, 1998
516.93	6.6	0.6	0.6	0.70897	Israelson and Spezzaferri, 1998
552.36	10.1	0.8	0.8	0.708927	Israelson and Spezzaferri, 1998
553.86	10.6	0.8	0.8	0.708915	Israelson and Spezzaferri, 1998
581.26	10	0.8	0.8	0.708931	Israelson and Spezzaferri, 1998
590.94	11	0.8	0.8	0.708903	Israelson and Spezzaferri, 1998
620.21	10.8	0.8	0.8	0.708908	Israelson and Spezzaferri, 1998
621.16	12	0.8	0.8	0.708878	Israelson and Spezzaferri, 1998
621.66	11.3	0.8	0.8	0.708894	Israelson and Spezzaferri, 1998
628	10.7			First occurrence N. acostanensis	Larsen, 1994
645	11.9			Last occurrence C. floridanus	Larsen, 1994
656.14	13.7	0.8	0.8	0.708832	Israelson and Spezzaferri, 1998
656.14	13.7	0.8	0.8	0.708833	Israelson and Spezzaferri, 1998
657	13.25	1.25	1.25	G. praemenardii range	Larsen, 1994
682.58	13.2	0.8	0.8	0.708846	Israelson and Spezzaferri, 1998
688	13.6			Last occurrence S. heteromorphus	Larsen, 1994
697.07	13	0.8	0.8	0.70885	Israelson and Spezzaferri, 1998
697.07	13.6	0.8	0.8	0.708835	Israelson and Spezzaferri, 1998
726.01	16.1	0.4	0.4	0.708757	Israelson and Spezzaferri, 1998
786.22	17.7	0.4	0.4	0.708647	Israelson and Spezzaferri, 1998
786.22	17.7	0.4	0.4	0.708648	Israelson and Spezzaferri, 1998
803.99	19.9	0.4	0.4	0.708496	Israelson and Spezzaferri, 1998
803.99	19.6	0.4	0.4	0.708519	Israelson and Spezzaferri, 1998
850.27	22.7	0.4	0.4	0.708303	Israelson and Spezzaferri, 1998
850.27	22.6	0.4	0.4	0.708314	Israelson and Spezzaferri, 1998
850.27	22.6	0.4	0.4	0.708311	Israelson and Spezzaferri, 1998

Israelson, C. & Spezzaferri, S. in *Proceedings of the Ocean Drilling Program, Scientific Results* **152** (eds A.D. Saunders, H.C. Larsen, & S.W. Wise, Jr.) 233-241 (1998).

Fukuma, K. in *Proceedings of the Ocean Drilling Program, Scientific Results* **152** (eds A.D. Saunders, H.C. Larsen, & S.W. Wise, Jr.) 265-269 (1998).

Larsen, H. C. *et al.* Seven million years of glaciation in Greenland. *Science* **264**, 952–955 (1994).